Continuously Delay-Time Tunable-Waveguide Hologram Module for X-Band Phased-Array Antenna

Zhong Shi, Yongqiang Jiang, Brie Howley, Yihong Chen, Feng Zhao, and Ray T. Chen, *Senior Member, IEEE*

***Abstract*—Tunable optical true time-delay modules based on a dispersive waveguide hologram are presented to provide continuous radio-frequency beam scanning for an X-band (8–12 GHz) phased-array antenna system. The true time-delay modules operating in the 1550-nm region were fabricated with continuously tunable time delays from 5 to 64 ps. The far-field radiation patterns were measured with different delay combinations and the continuity of the scanning angles from 35° to 55° was experimentally confirmed at X-band frequencies.**

***Index Terms*—Grating dispersion, optical true time delay, phased-array antenna, wavelength tuning.**

I. Introduction

THE PHASED-ARRAY antenna is one of the key technologies in modern radar and communication systems. It offers advantages such as quick and accurate radio-frequency (RF) beam scanning without physical movement, reduced weight, and less power consumption. true time-delay techniques are used in phased-array antenna systems to overcome the frequency squint effect that causes the undesired changing of the beam-scanning angle. Compared with electrical true time-delay techniques, optical true time-delay techniques have better performance in bandwidth and electromagnetic interference [1], [2]. A waveguide-hologram-based optical true time-delay technique has been drawing lots of attention due to the advantages of easy fabrication and large packaging density [3]–[5]. However, the time delays provided by [3] and [4] are only partially continuous. Although [5] proposed a pseudoanalog true time-delay scheme, it is difficult to get wide continuous-tuning time delays with this scheme due to the requirement of very large wavelength tuning range up to hundreds of nanometers.

It is desirable to provide continuous-tuning time delays with the operating wavelength in 1550-nm region, considering its real application in a phased-array antenna system. In this letter, we present an improved wavelength-tuning method in waveguide-hologram true time-delay modules to provide continuous RF beam scanning for an X-band (8–12 GHz) phased-array antenna system. The true time-delay modules reported herein can provide continuous time delays from 5 to 64 ps. These modules were fabricated for use in the 1550-nm wavelength region, which is compatible with the transparent transmission window of optical communications.

Manuscript received November 27, 2002; revised March 28, 2003. This work was supported by the Airforce Office of Scientific Research and the MDA.

The authors are with the Department of Electrical and Computer Engineering, Microelectronics Research Center, The University of Texas at Austin, Austin, TX 78758 USA (e-mail: raychen@uts.cc.utexas.edu).

Digital Object Identifier 10.1109/LPT.2003.813392

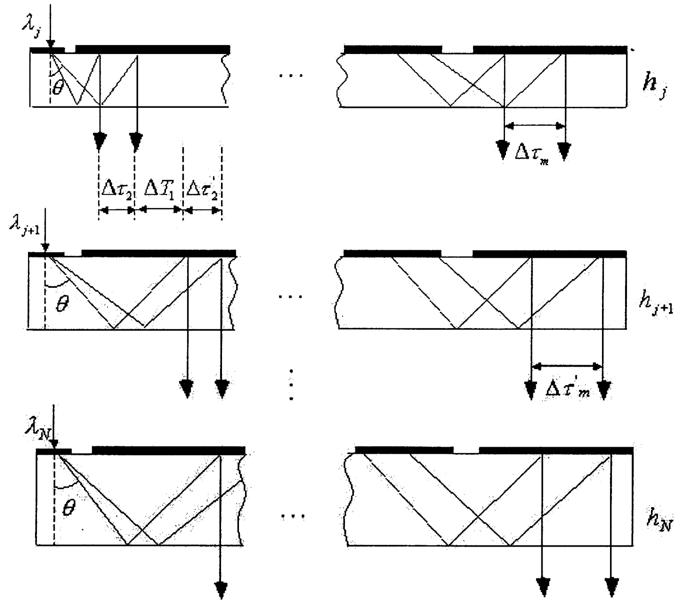

Fig. 1. Configuration of the wavelength-tuning hologram waveguide-based true time-delay modules, consisting of N discrete glass waveguide strips of thicknesses $h_1, h_2, \ldots, h_N$, each with the same hologram grating structure on its top surface. Continuous time delays are achieved by tuning wavelengths in the different time-delay modules.

II. Principle

The general configuration of the proposed wavelength-tuning scheme is shown in Fig. 1. The system has N discrete waveguide stripes with thicknesses of $h_1, h_2, \ldots$, and h_N, respectively. They are controlled independently by N discrete wavelengths, $\lambda_1, \lambda_2, \ldots, \lambda_N$. All waveguide stripes have the same hologram grating structure on the top surface to provide surface-normal fanouts. Therefore, all diffracted beams have the same diffraction angle θ in all modules when the incident beams have the same wavelength. The $(m+1)$th fanouts (m: bouncing number in the substrate) between the jth module and the $(j+1)$th module have a time delay ΔT_{m+1} at the incident center wavelength λ. If the incident wavelength for the jth module is tuned from center wavelength λ to $\lambda + \Delta\lambda$, the diffraction angle

TABLE I
DESIGNED TRUE-TIME-DELAY RESULTS AT DIFFERENT INCIDENT WAVELENGTHS. THE TIME DELAYS ARE CONTINUOUS FROM 5 TO 64 ps ACROSS THE WAVELENGTH-TUNING RANGE

Fan out No.	Minimum time delays (ps) at $\Delta\lambda_1 = 50nm$ $\Delta\lambda_2 = -50nm$	Minimum time delays (ps) at $\Delta\lambda_1 = 30nm$ $\Delta\lambda_2 = -30nm$	Time delays (ps) at 1550nm $\Delta\lambda_1 = 0nm$ $\Delta\lambda_2 = 0nm$	Maximum time delays (ps) at $\Delta\lambda_1 = -30nm$ $\Delta\lambda_2 = 30nm$	Maximum time delays (ps) at $\Delta\lambda_1 = -50nm$ $\Delta\lambda_2 = 50nm$
1	2.205	2.205	2.205	2.205	2.205
2	5.435	6.575	8.235	9.895	11.035
3	8.665	10.945	14.265	17.585	19.865
4	11.895	15.314	20.295	25.276	28.695
5	15.125	19.744	26.325	32.966	37.525
6	18.355	24.053	32.355	40.657	46.355
7	21.584	28.420	38.384	48.348	55.184
8	24.810	32.789	44.414	56.039	64.018

becomes $\theta + \Delta\theta$ and $\Delta\theta$ is determined by the dispersion equation which is derived from the Bragg condition [6]

$$\Delta\theta = 2\frac{\Delta\lambda}{\lambda}\tan\left(\frac{\theta}{2}\right). \quad (1)$$

This introduces a time delay $\Delta\tau$ between λ and $\lambda + \Delta\lambda$ for the $(m+1)$th fanout in the module j. $\Delta\tau_{m+1}$ is determined by

$$\Delta\tau_{m+1} = \frac{2mnh_j}{c}\left[\frac{1}{\cos(\theta+\Delta\theta)} - \frac{1}{\cos(\theta)}\right]. \quad (2)$$

Here n is the refractive index of the glass substrate. When the wavelength is tuned from λ to $\lambda + \Delta\lambda'$ in the $(j+1)$th module, the diffracted beam $\lambda + \Delta\lambda'$ has a diffraction angle of $\theta + \Delta\theta'$ and $\Delta\theta'$ is also determined by (1). The time delay $\Delta\tau'_{m+1}$ between λ and $\lambda + \Delta\lambda'$ for the $(m+1)$th fanout in the $(j+1)$th module is determined by the same equation as (2) except substrate thickness h_j is replaced by h_{j+1}. The total time delay $\Delta T'_{m+1}$ for the $(m+1)$th fanout between the adjacent modules can be continuously tuned as the following equation depending on the wavelength tuning direction in the different modules:

$$\begin{aligned}\Delta T_{m+1} - (\Delta\tau_{m+1} + \Delta\tau'_{m+1}) &\le \Delta T'_{m+1}\\ &\le \Delta T_{m+1} + (\Delta\tau_{m+1} + \Delta\tau'_{m+1}).\end{aligned} \quad (3)$$

For the time delays to be continuously tuned in the devices, the maximum time delay from the mth output has a fanout equal to or larger than the minimum time delay from the $(m+1)$th output. Then the following equation should be satisfied:

$$\Delta T_m + (\Delta\tau_m + \Delta\tau'_m) \ge \Delta T_{m+1} - (\Delta\tau_{m+1} + \Delta\tau'_{m+1}). \quad (4)$$

With different delay combinations, the proposed scheme is capable of generating continuous time delays for RF beam scanning. Equation (4) is used to design such parameters of the true time-delay modules as the diffraction angle at the center wavelength 1550 nm, thickness difference between modules, and the total bouncing number in the substrates. These parameters should be considered together in the design work. Table I shows the designed time-delay result for the different fanouts at the different tuning wavelengths for the two stripes $(N = 2)$ having eight fanouts each. The results in Table I show that the time delay is continuous from 5 to 64 ps within the wavelength tuning range. The scanning angle θ of an antenna can be computed from

$$\sin\theta = \frac{c\Delta T}{d} \quad (5)$$

where c is light speed, ΔT is time delay, and d is the distance between adjacent radiating elements which is 2 cm for our case. The designed beam-scanning angle can be tuned from 4.3° to 73°.

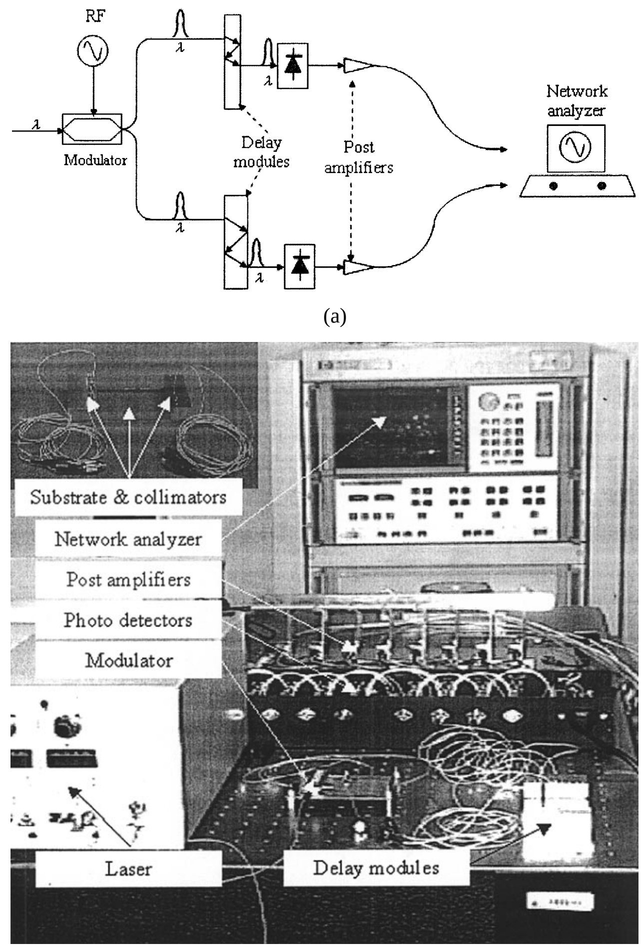

(a)

(b)

Fig. 2. (a) Experimental setup block diagram for measuring the time delays. (b) Photo of the experimental system.

III. EXPERIMENTAL RESULTS

To reduce the module size and get sufficient continuous time delays for an X-band phased-array antenna system, a diffraction angle of 43° was chosen at the center wavelength of 1550 nm. Using (1), we can get $\Delta\theta = \pm 0.874°$ for $\Delta\lambda = \pm 30$ nm and $\Delta\theta = \pm 1.457°$ for $\Delta\lambda = \pm 50$ nm. Two modules having thickness of 4.041 and 4.482 mm were fabricated. The length of the each module was chosen to provide eight fanouts ($m = 0, \ldots, 7$, in our case). To verify the designed result of time delay, we used the experimental setup shown in Fig. 2(a) to measure the RF phase versus RF frequency curves. An HP network analyzer (8510C) was used to provide an X-band RF signal and

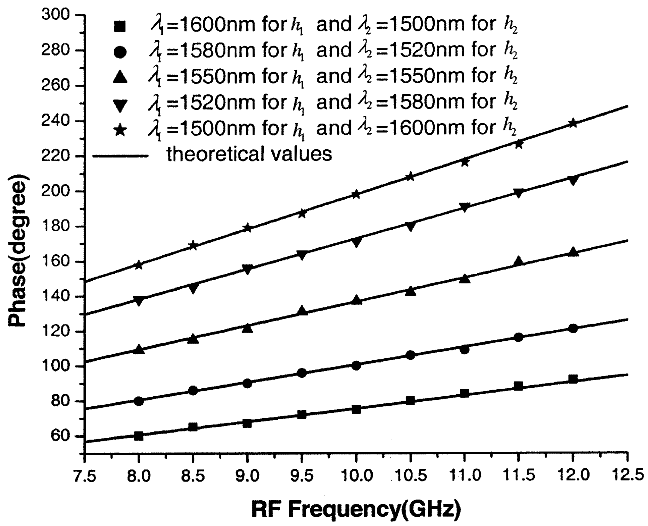

Fig. 3. Measured results and simulated results of RF phase versus RF frequency covering X-band. The time delays can be calculated from the slope of each curve.

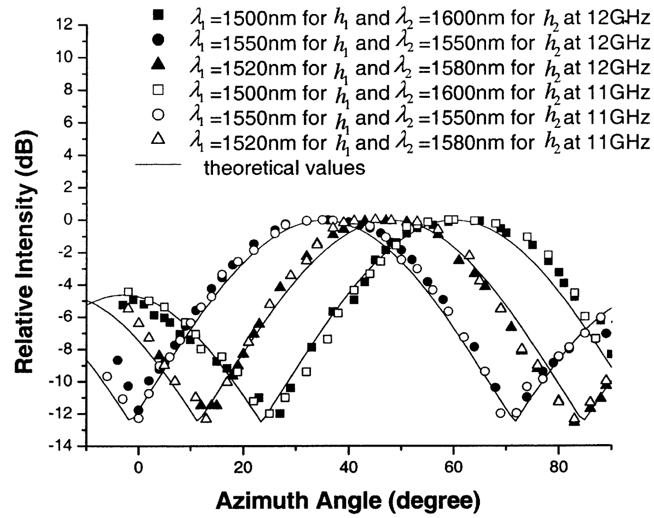

Fig. 4. Measured and simulated radiation patterns at 11 and 12 GHz under different tuning wavelengths.

to measure the time delays in the experiment. A Santec tunable laser was modulated by a $LiNbO_3$ external modulator and the modulated signal was fed into one of the true time-delay modules h_1(4.041 mm) or h_2(4.482 mm). After the desired time delays within the module, the output was fed into the high-speed p-i-n photodetector connected with postamplifier (PA). The phase of the electrical signal from the PA was measured by the HP network analyzer. Fig. 2(b) is a photo of the system structure. We measured the seventh $(\mathrm{m} = 6)$ fan-out for both modules in the experiment. The results of RF phase versus RF frequency are shown in Fig. 3. The time delays obtained from the above measurement are 21 ps at $\lambda_1 = 1600$ nm for h_1 and $\lambda_2 = 1500$ nm for h_2, 28 ps at $\lambda_1 = 1580$ nm for h_1 and $\lambda_2 = 1520$ nm for h_2, 38 ps at $\lambda_1 = 1550$ nm for h_1 and $\lambda_2 = 1550$ nm for h_2, 48 ps at $\lambda_1 = 1520$ nm for h_1 and $\lambda_2 = 1580$ nm for h_2, and 55 ps at $\lambda_1 = 1500$ nm for h_1 and $\lambda_2 = 1600$ nm for h_2. The measured time delays are independent of RF frequency as it can be confirmed through the linearity of RF phase versus RF frequency curves shown in Fig. 3.

To further verify the functionality of the designed modules, the radiation patterns of the two radiating elements were measured across RF X-band range. The measurement was made in the E-plane that corresponded to the maximum radiation direction of the antenna. The measured radiation patterns at 11 and 12 GHz are shown in Fig. 4. The void spots represent the measurement made at 11 GHz and the black spots represent the measurement made at 12 GHz. The circles represent measurements at $\lambda_1 = \lambda_2 = 1550$ nm for both modules, which gives a beam-scanning angle at 35°. The triangles were measured with $\lambda_1 = 1520$ nm for h_1 and $\lambda_2 = 1580$ nm for h_2 corresponding to the beam-scanning angle at 46° and the squares were measured with $\lambda_1 = 1500$ nm for h_1 and $\lambda_2 = 1600$ nm for h_2 corresponding to the beam-scanning angle at 55°. As expected, no beam squint was found in the experiment. The first null depth is more than 12 dB for the patterns in Fig. 4. The simulated results are shown with solid lines for comparison. The simulation was made for a notched antenna used in the experiment at 12 GHz [7]. Using different fanout combinations can cover all the designed angles in the experiment. By employing more modules, narrower far-field RF beam width can be achieved.

IV. Conclusion

We have proposed an idea of using dispersive waveguide hologram-based true time-delay modules to provide continuous RF beam scanning for an X-band phased-array antenna system. The designed time delays can be continuously tuned from 5 to 64 ps. The measured time delays agree well with the designed values. The radiation patterns across the X-band were measured and the results were shown at 11 and 12 GHz.

Acknowledgment

The authors would like to thank Dr. J. Pohlmann and Dr. C. Lee for their support and encouragement.

References

[1] D. Dolfi, J. P. Huignard, and M. Baril, "Optically controlled true time delays for phased array antenna," *Proc. SPIE*, vol. 1102, pp. 152–161, 1989.
[2] W. Ng, A. A. Walston, G. L. Tangonan, J. J. Lee, I. L. Newberg, and N. Bernstain, "The first demonstration of an optically steered microwave phased array antenna using true time-delay," *J. Lightwave Technol.*, vol. 9, pp. 1124–1131, Sept. 1991.
[3] R. Li, Z. Fu, and R. Chen, "High packing density 2.5 THz true time-delay lines using spatially multiplexed substrate guided waves in conjunction with volume holograms on a single substrate," *J. Lightwave Technol,*, vol. 15, pp. 2253–2258, Dec. 1997.
[4] Y. Chen and R. T. Chen, "A fully packaged true time delay modules for a K-band phased array antenna demonstration," *IEEE Photon. Technol. Lett.*, vol. 14, pp. 1175–1177, Aug. 2002.
[5] Z. Fu, C. Zhou, and R. T. Chen, "Waveguide-hologram-based wavelength-multiplexed pseudoanalog true time-delay module for wideband phased-array antennas," *Appl. Opt.*, vol. 38, no. 14, pp. 3053–3059, 1999.
[6] H. Kogelnik, "Coupled wave theory for thick hologram gratings," *Bell Syst. Tech. J.*, vol. 48, pp. 2909–2947, 1969.
[7] J. A. Navarro and K. Chang, *Integrated Active Antennas and Spatial Power Combining*. New York: Wiley, 1996.